The electrorheological behaviour of suspensions based on molten-salt synthesised lithium titanate nanoparticles and their core-shell titanate/urea analogues

Plachy T.[a,b], Mrlik M.[a], Kozakova Z. [a], Suly P. [a,b], Sedlacik M. [a*], Pavlinek V.[a], Kuritka I.[a]

[a] *Centre of Polymer Systems, University Institute, Tomas Bata University in Zlin, Nad Ovcirnou 3685, 760 01 Zlin, Czech Republic*

[b] *Polymer Centre, Faculty of Technology, Tomas Bata University in Zlin, Nam. T. G. Masaryka 275, 762 72 Zlin, Czech Republic*

**e-mail address: msedlacik@ft.utb.cz*

Abstract

This paper concerns the preparation of novel electrorheological (ER) materials using microwave-assisted synthesis as well as utilizing a suitable shell-providing system with enhanced ER performance. Lithium titanate nanoparticles were successfully synthesised and their composition was confirmed via X-ray diffraction. Rheological properties were investigated in the absence as well as in the presence of an external electric field. Dielectric properties clarified the response of the particles to the application of an electric field. The urea-coated lithium titanate nanoparticle-based suspension exhibits higher ER performance in comparison to suspensions based on bare particles.

KEYWORDS: Electrorheology, microwave-assisted molten-salt synthesis, anatase, lithium titanate, dielectric properties, steady shear

1. Introduction

Electrorheological (ER) suspensions are generally two-phase systems consisting of polarizable particles suspended in an insulating carrier liquid, mostly silicone oil. Such particles are able to create induced dipoles and to form internal chain-like structures after the application of an external electric field. Such structure development results in the transition from a liquid to solid-like state connected to a viscosity increase of several orders of magnitude (1-8). Hence, ER suspensions have been increasingly applied to the smart control of intelligent as well as conventional devices, as shock absorbers, clutches and other applications. (9-11).

Commonly, the dispersed phase is represented by conducting polymers (12-18) or inorganic particles (19-23). In the case of inorganic particles, many researchers have focused on the synthesis and ER investigation of titanate-based ER suspensions (24-27). Titanates are preferred due to their high relative permittivity and nanoparticles size contributing to enhanced ER efficiency and substantially-improved sedimentation stability (27, 28).

Titanates are mostly prepared by solvothermal synthesis using strong solvents, and reaction times are in the order of hours or days (24, 26). Such procedures are considerably time-consuming and harmful to the environment. On the other hand, molten-salt microwave-assisted synthesis provides a possible way to prepare suitable particles for ER suspensions due to the short reaction times and solvent-free and thus environmentally-friendly procedure (29, 30). It has been demonstrated that using a molten salt synthesis, the particle size depends on the temperature and time of a synthesis (31, 32). Usually, the particle size increases with prolonging synthesis time and increasing synthesis temperature.

Hence, this study is focused on the synthesis of lithium titanate (Li-titanate) nanoparticles from titanium dioxide (TiO_2 anatase) nanoparticles via molten-salt microwave-assisted synthesis. The synthesis time was chosen in order to prepare nanoparticles, since nanoparticles exhibit higher sedimentation stability than micron-sized particles. Moreover, the prepared particles were coated with urea in order to improve ER performance. Then the rheological properties of the anatase, Li-titanate, and urea-coated Li-titanate-based ER suspensions were investigated in the absence and presence of an external electric field. The interfacial polarization mostly responsible for the ER effect was then evaluated through a dielectric property examination.

2. Experimental

2.1. Synthesis of Lithium Titanate nanoparticles

Li-titanate particles were prepared by molten-salt synthesis without the use of any solvent. A mixture of reactants, i.e., 1 g of TiO_2 anatase, 2.47 g of lithium chloride and 1.53 g of lithium carbonate (all purchased from Sigma Aldrich, USA), was homogenized in a mortar and inserted into a corundum crucible. The filled crucible was placed into a special ceramic kiln, the inner walls of which were coated with graphite. Then the kiln was put into a common domestic microwave oven working at frequency 2.45 GHz and a maximum power of 750 W. The reacting mixture was treated for 20 minutes at maximum power and then allowed to cool down to room temperature inside the closed ceramic kiln. Then, the obtained compact solid product was rinsed with demineralized water, filtered off and then washed with demineralized water again. The

product was labeled as Sample 1 (S1) and then dried in an oven under vacuum at 60 °C to a constant weight.

2.2. Treatment of S1 particles in urea solution

The prepared S1 particles (1.5 g) were immersed in 50 ml of demineralized water at 45 °C. After 1 h, 1.5 ml of 10 wt% aqueous solution of urea (Sigma Aldrich, USA) was added. The mixture was stirred for another 16 h. Subsequently, the suspension was filtered and rinsed with demineralized water. The obtained particles were dried in a vacuum oven at 60 °C to a constant weight. These particles were then labeled as Sample 2 (S2).

2.3. Characterization of prepared nanoparticles

The morphology and dimensions of the particles were observed using transmission electron microscopy (TEM; Tesla 500, Czech Republic). The chemical composition of the prepared titanate particles was characterized with the use of X-Ray diffraction (XRD) analysis. The diffraction pattern of the prepared material was examined using an X-pert PRO (Phillips, The Netherlands) diffractometer with a Cu $K_{\alpha 1}$ radiation (λ = 0.154 nm) and a scanning rate 4 min^{-1} in an angle range of 10–95° 2θ. In order to confirm the presence of urea in the S2 and to determine its amount, Fourier transform infrared spectra were measured via the ATR method with a diamond crystal in a range from 4000–500 cm^{-1} on a Nicolet 6700 (Nicolet, USA). A thermogravimetric analysis (TGA; TGA Q500; TA Instruments, USA) was also made. The TGA measurement was performed at a heating rate 5 °C min^{-1} from 25 °C to 400 °C under a nitrogen atmosphere.

TEM images (Fig. 1 a-c) show agglomerates of (a) the precursor material TiO_2 anatase, (b) the prepared S1 and (c) the prepared S2. The particles possess a spherical-like shape with a diameter in the range between tens of nanometres up to 150 nm indicating, that samples S1 and S2 belong to the group of nanoparticles. It can be seen that the prepared S1 and S2 particles have similar dimensions as the TiO_2 anatase particles.

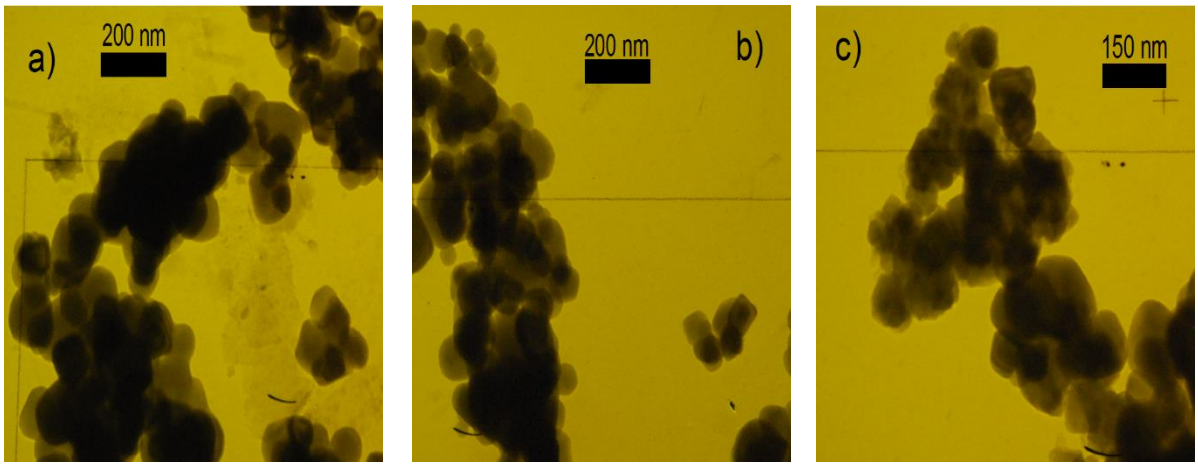

Fig. 1 TEM images for (a) TiO_2 anatase, (b) S1 and (c) S2 particles.

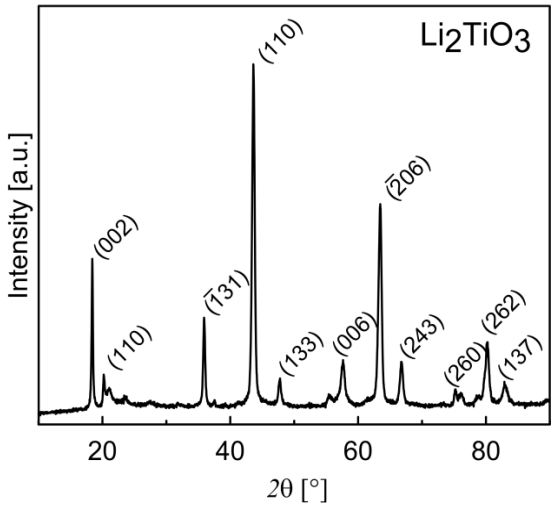

Fig. 2 Powder XRD pattern of synthesized S1 particles.

On the basis of a comparison with the ICDD PDF-2 database, the prevailing crystallographic phase present in the sample was identified as Li_2TiO_3 (Fig. 2). The compound Li_2TiO_3 crystallizes in three structural modifications, cubic α-Li_2TiO_3 (space group Fm-3m), which is metastable and above 300 °C transforms irreversibly into the monoclinic β-Li_2TiO_3 (space group C2/c). The monoclinic phase is stable in a wide temperature range up to 1150 °C, after which cubic γ-Li_2TiO_3 (space group Fm-3m) occurs. The diffraction patterns of the monoclinic and cubic crystallographic phases contain several peaks presented in the same position; however, the complex character of the diffraction pattern of S1 presented in Fig. 2 contains diffraction peaks in the range of 2θ angles from 20-24°, which are specific just for the monoclinic phase and thus indicate the presence of this phase in the prepared material. This can

also be supported by the fact that the temperature of synthesis is assumed to be in the range of about 600-800 °C, in which the monoclinic phase is stable.

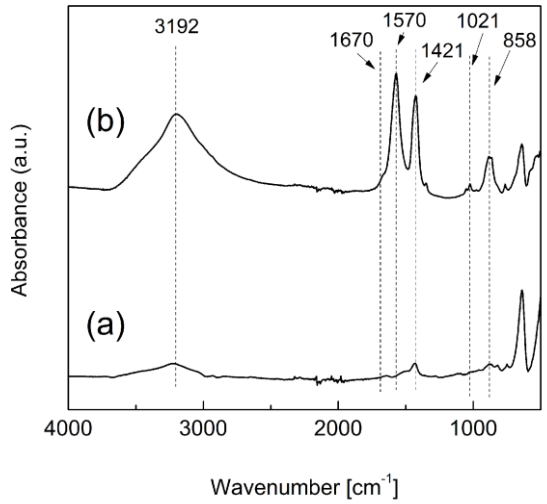

Fig. 3 FTIR spectra for S1 (a) and S2 (b).

In Fig. 3, the FTIR spectra of the bare S1 particles and also the particles after urea coating can be seen. The particles before coating (S1) exhibit typical stretching vibrations for –OH groups at 3200 cm^{-1} and typical vibrations at 1421 and 858 cm^{-1} and lower for TiO_3 bands (33). Further, in the case of urea-modified particles (S2), the typical N-C-N asymmetric and symmetric stretching vibrations at 1421 and 1021 cm^{-1} are presented, respectively. Also the C=O stretching and N-H bending appear at 1670 and 1570 cm^{-1} (34). The broad band at 3192 cm^{-1} can be attributed to the N-H stretching and/or O-H stretching in adsorbed water. The broadening of this peak can be also assigned to the enhanced interaction of the S1 with urea by hydrogen bonding, as was also observed by Cheng et al. (35).

The presence of urea on the surface of S1 after its treatment was also confirmed by TGA. The TGA curve for S2 (Fig. 4) exhibits a similar shape to the curve obtained for pure urea (36). The highest mass loss was observed in the temperature region around 150–260 °C. By TGA analysis, it was confirmed that the amount of urea present in S2 was 1.86 %. The first step may be attributed to the partial decomposition of urea to isocyanic acid and ammonia. The less developed peak in DTGA and the low loss of mass above the temperature 260 °C represents residual byproducts of urea decomposition like ammelide or cyanuric acid. The further decrease in mass represents the decomposition of cyanuric acid (36). It is also seen that bare S1 particles are stable up to 400 °C, and the mass change is significantly smaller in comparison with S2.

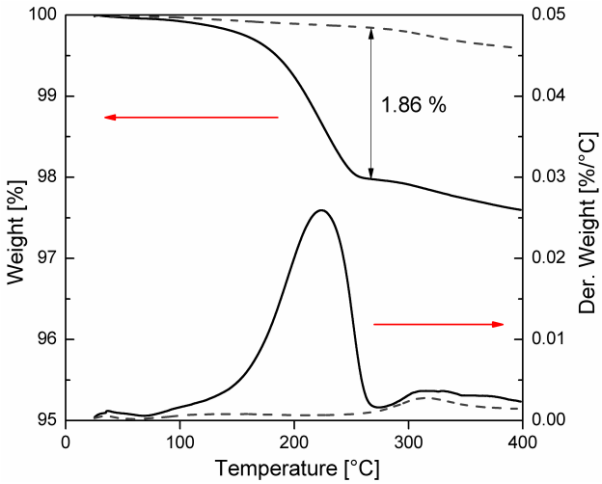

Fig. 4 TGA analysis of S1 (dashed line) and S2 (solid line) samples.

2.4. Preparation of electrorheological suspensions

The prepared particles were dried in a vacuum oven at 60 °C for 24 h. Subsequently, ER suspensions of concentration 5 wt%, 10 wt%, and 15 wt% were prepared by mixing the dried particles with silicone oil (Lukosiol M200, Chemical Works Kolín, Czech Republic, viscosity η_c = 194 mPa s, conductivity $\sigma_c \approx 10^{-11}$ S cm^{-1}), which were then dried under the same conditions. The suspensions were stirred manually for 5 min and then sonicated for 1 min before each measurement.

2.5. Electrorheological measurements

Steady shear measurements in controlled shear rate mode were carried out using a Bohlin Gemini rotational rheometer (Malvern Instruments, UK) with parallel plate geometry 40 mm in diameter and a gap of 0.5 mm. A DC TREK 668B high-voltage source (TREK, USA) was used for the generation of external electric fields of strength 0–3 kV mm^{-1}. Before each measurement, the suspension was sheared for 60 s at a shear rate of 40 s^{-1} in order to destroy residual chain-like structures. In the case of measurements in the presence of an electric field, the electric field was applied for 60 s before shearing to provide enough time for particles to create organized structures within the suspensions.

2.6. Dielectric properties

Dielectric properties of prepared suspensions were measured with an impedance analyser (4294A, Agilent Technologies, Japan) connected to a cell for liquid materials (16482A, Agilent Technologies, Japan). Dielectric properties such as relative permittivity, ε', and dielectric loss factor, ε'', were investigated in a frequency range from 60 Hz to 2 MHz. Dielectric spectra were analyzed using the Havriliak-Negami (H-N) model (37),

$$\varepsilon^*_{HN}(\omega) = \varepsilon'_{\infty} + \frac{\Delta\varepsilon'}{\left(1 + (i\omega \cdot t_{rel})^a\right)^b} \quad (1)$$

where $\Delta\varepsilon' = \varepsilon'_s - \varepsilon'_\infty$ is the dielectric relaxation strength, ε'_s, and ε'_∞, are the relative permittivities at zero and infinite frequency, f, respectively, and ω is the angular frequency ($=2\pi f$), t_{rel} is the relaxation time, and a and b are shape parameters describing the asymmetry of the dielectric function.

2.7. Optical microscopy

Suspensions consisting of 1 wt% of particles in silicone oil were placed between two copper electrodes deposited on a glass (gap of 1 mm) connected to a DC high-voltage source (Keithley 2400, USA). The formation of ER structures was observed with the help of an optical microscope (N 400M, China) linked to a digital camera.

3. Results and Discussion

3.1. Electrorheological properties

The ER performance of 5 wt% suspensions based on TiO_2 anatase and S1 was investigated in the absence and in the presence of an electric field. As can be seen in Fig. 5, the suspensions exhibit Newtonian behavior in the absence of an electric field, and their field-off viscosity is similar. However, in the presence of an electric field of a strength of 3 kV mm^{-1}, the S1-based suspension shows a higher yield stress than the anatase-based suspension due to the increased polarizability of the S1 particles. At shear rates above 10 s^{-1}, the shear stress of both suspensions started to exhibit values regardless whether the external electric field is applied or not (Fig. 5). The values of shear stress of ER suspensions in the presence of external electric field are determined by the ratio of electrostatic and hydrodynamic forces. Since the loading of the suspensions is only 5 wt%, the electrostatic forces are weak and hydrodynamic ones start to dominate over them at quite low shear rates. Similar values of shear stress were then obtained

due to similar particles size of both suspensions. Very similar behavior has been observed with an ER suspension based on particles of low conductivity (38, 39).

Due to the increased yield stress, the S1 sample seems to be a more promising material for a highly effective ER fluid in comparison with the TiO_2 anatase. These findings were also confirmed via observation of the structure development under the application of an external electric field (see chapter, Structure Development under DC Electric Field). The S1 particles were therefore further treated in urea solution in order to improve the ER performance of their silicone oil suspensions.

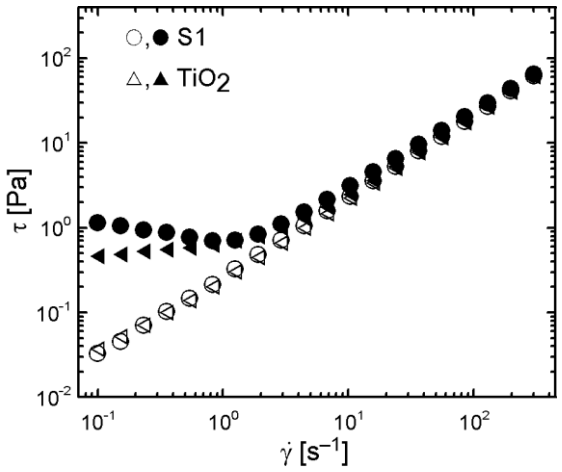

Fig. 5 Dependence of shear stress, τ, on shear rate, $\dot{\gamma}$, for 5 wt% ER suspensions based on TiO_2 anatase and S1 particles in the absence (open symbols) and in the presence of an external electric field of a strength of 3 kV mm^{-1} (solid symbols).

Fig. 6 shows the ER performance of suspensions containing various concentrations of S2 particles. The suspension containing 5 wt% particles behaves as a Newtonian fluid in the absence of an electric field and exhibits higher yield stress at the same electric field strength than the suspension based on S1 particles in Fig. 5. Thus, the introduction of a polar layer on the surface of S1 led to an increase in the ER effect of the suspension. The suspensions based on 10 wt% and 15 wt% particles behave rather like pseudoplastic fluids than Newtonian ones in the absence of an electric field. However, upon the application of an external electric field strength of 3 kV mm^{-1}, both begin to act as Bingham fluids exhibiting considerable high yield stresses. The higher particle concentration in the suspensions led to a significant increase in the ER effect of these suspensions; the particles were able to create stiffer and tougher chain-like structures than in the case of suspensions with a low loading of the particles.

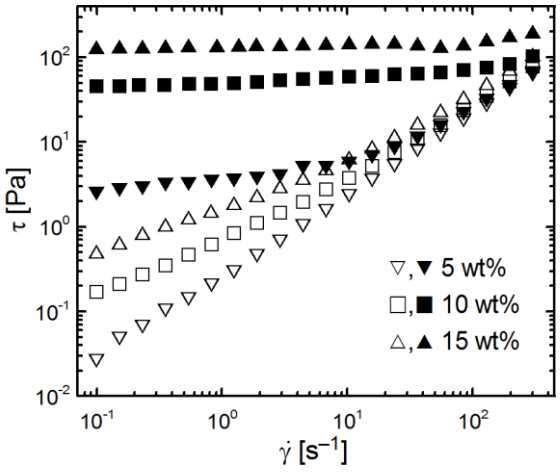

Fig. 6 Dependence of shear stress, τ, on shear rate, $\dot{\gamma}$, for the ER suspensions based on the various concentrations of S2 in the absence (open symbols) and in the presence of an external electric field of a strength of 3 kV mm^{-1} (solid symbols).

It was proposed that the log-log dependence of the yield stress on the electric field strength (Fig. 7) obeys the power law

$$\tau = q \times E^{\alpha} \tag{2}$$

where q represents the rigidity of the internal structures created upon the application of the electric field and the value of parameter α should be within the range 1.5-2 for well-developed structures (40, 41). However, since it is complicated to exactly determine the yield stress, the values of shear stress at a very low shear rate of 0.1 s^{-1} were taken for this evaluation. In the case of suspensions based on 15 wt% and 10 wt% S2 particles, their parameters α possess values 1.87 and 1.70, respectively. This indicates better developed structures upon application of the external electric field for the higher loaded suspension. Thus, the increased amount of polarizable particles leads to the creation of a stiffer system exhibiting a higher ER effect. For the suspension based on 5 wt% S2 particles, α parameter is only 1.15, which corresponds well with the low ER effect of this suspension.

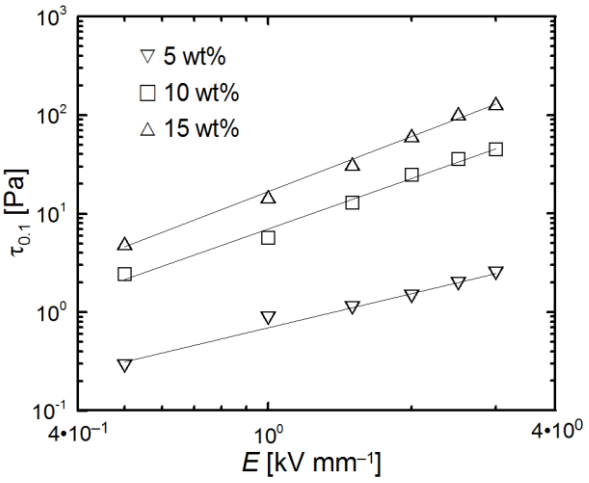

Fig. 7 The values of the shear stress obtained at the shear rate 0.1 s^{-1} vs. the electric field strength for the ER suspensions based on various concentrations of S2.

From the application point of view, the difference between viscosity in the presence of an external electric field, η_E, and viscosity in the absence of an electric field, η_0, is of high importance. This difference is embodied in the formula of ER efficiency, *e*, where

$$e = (\eta_E - \eta_0)/\eta_0 \quad (3)$$

Fig. 8 shows the dependence of ER efficiency on the shear rate for the S2 sample suspensions. Despite the highest field-off viscosity, the suspension based on 15 wt% S2 particles exhibits the highest ER efficiency together with the suspension based on 10 wt% S2 particles. However, it can be seen that at higher shear rates than 10^{-1} s, a higher efficiency for the suspension based on 15 wt% S2 particles is observed. This is a consequence of the changes in the field-off viscosity with increasing shear rates. The higher loaded suspension behaves more like a pseudoplastic fluid; thus, its viscosity is significantly higher than the viscosity of the suspension containing 10 wt% S2 particles. However, at shear rates higher than 10^{-1} s, the difference significantly decreases and is similar for both suspensions, which leads to the higher efficiency of the suspension based on 15 wt% S2 particles due to its higher ER effect. The suspension based on 5 wt% S2 particles, which possesses the lowest field-off viscosity, exhibits also the lowest ER efficiency. This corresponds well with its ER effect (lower more than one order of magnitude) in comparison with both higher-loaded suspensions. It can also be assumed that a further increase in the concentration of S2 particles in the suspensions would not lead to an ER fluid with higher ER efficiency owing to the high increase of field-off viscosity.

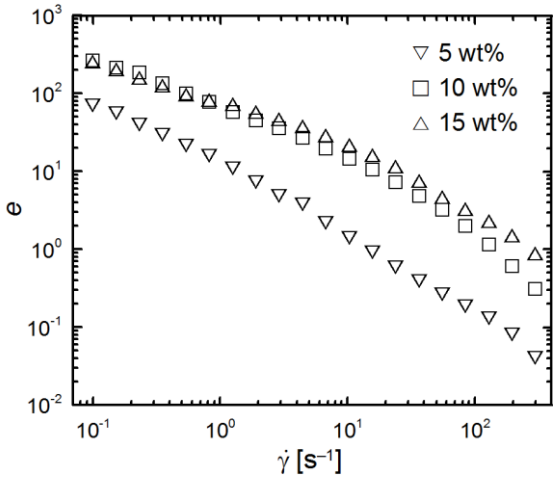

Fig. 8 The dependence of the ER efficiency, *e*, on the shear rate, $\dot{\gamma}$, for the ER suspensions based on the various concentrations of S2.

3.2. Dielectric properties

Generally, interfacial polarization is mostly responsible for the formation of the internal structures in the ER suspensions (42-45). In the dielectric spectra (Fig. 9), the presence of the relaxation peaks of both S1 and S2 5 wt%-based suspensions can be clearly seen. From an investigation of these spectra by an H-N model fit, the suitability of the synthesized S1 and S2 nanoparticles as dispersed phases in ER suspensions can be evaluated. The parameters of H-N model fits are shown in Table 1. Relaxation time t_{rel} and dielectric relaxation strength $\Delta\varepsilon'$ are the most important. Here the relaxation time reflects the rate of the interfacial polarization, which is on the same level for both investigated systems. However, dielectric relaxation strength as a measure of the electrostatic interactions between particles is two times higher for the S2-based suspension. Hence, the introduction of polar urea groups on the surface of S1 provides particles with higher polarizability, and their suspensions exhibit enhanced ER performance.

Table 1 Parameters of the Havriliak-Negami model fit for the 5 wt% suspensions of S1 and S2 nanoparticles.

Sample name	ε'_s	ε''_∞	$\Delta\varepsilon'$	t_{rel} [s]	a	b
S1	3.01	2.91	0.10	$1.15\ 10^{-3}$	0.66	0.59
S2	3.11	2.91	0.20	$1.49\ 10^{-3}$	0.61	0.68

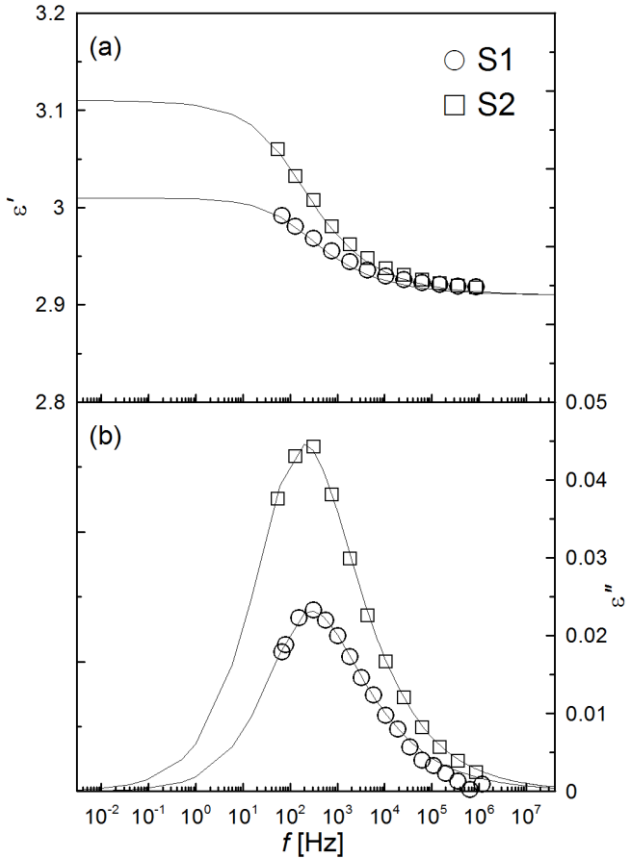

Fig. 9 The frequency dependence of relative permittivity, ε', (a) and dielectric loss factor, ε'', (b), for 5 wt% silicone oil ER suspensions. Solid lines represent the Havriliak-Negami model fit.

3.3. Structure development under DC electric field

In order to properly investigate the internal structure formation under the presence of an external electric field, the micrographs of structures (Fig. 10 and Fig. 11) were analysed. Since the small particles with high surface areas possess high surface energy, they tend to join together in bigger agglomerates; therefore, it was possible to investigate their structure by optical microscopy. The small amount of the original TiO_2 anatase agglomerates is randomly dispersed in the absence of an external electric field (Fig. 10a). After the application of the external electric field of 1.5 kV mm^{-1}, the TiO_2 anatase agglomerates are concentrated around the electrodes, and only large agglomerates developing defective structures are partially oriented (Fig. 10b). On the other hand, S1 small agglomerates randomly dispersed in silicone oil in the absence of an external field (Fig. 11a) are able to create considerably better developed internal structures after the application of the same electric field strength (Fig. 11b). Created agglomerates form visible chain-like internal structures and consequently provide enhanced ER activity well-reflected in the rheological behaviour. The highest ER activity was observed for the suspension based on S2. The particles are also randomly dispersed in the silicone oil in the absence of an external

electric field (Fig. 12a). However, after its application the particles undergo a transition to highly-organized, oriented, chain-like structures in the direction of the applied electric field (Fig. 12b). The resulting structures are obviously better formed than in the previous cases due to their enhanced dielectric relaxation strength. Therefore, the suspension based on S2 exhibits the highest ER effect among these suspensions.

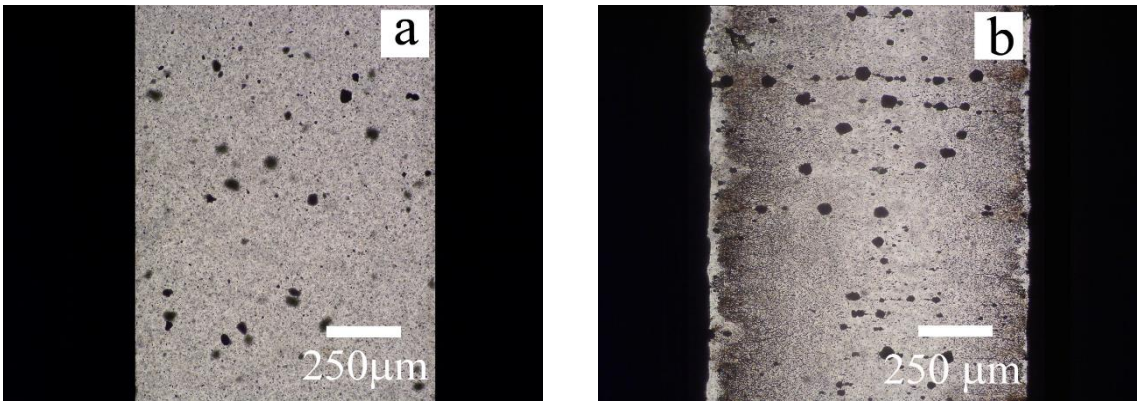

Fig. 10 Optical microscopy of a 1 wt% silicone oil suspension of TiO_2 anatase nanoparticles under various electric field strengths, *E*, (kV mm^{-1}): (a) 0, (b) 1.5.

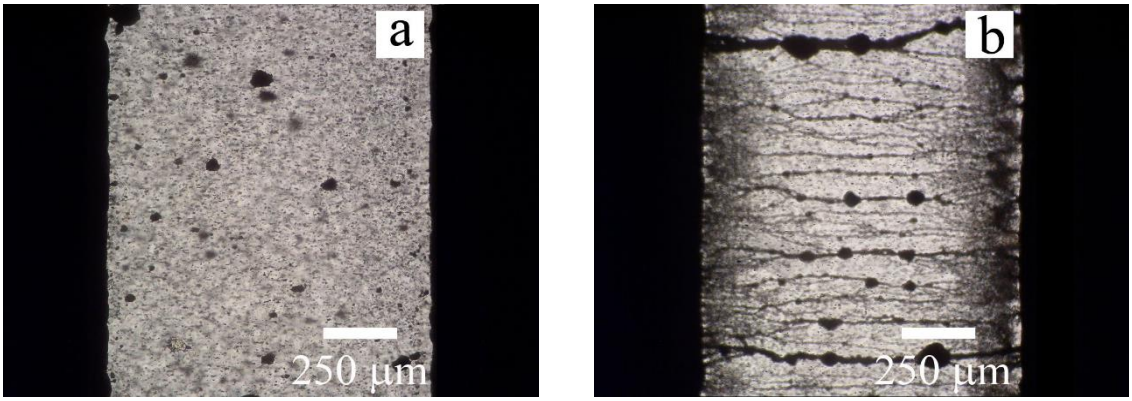

Fig. 11 Optical microscopy of a 1 wt% silicone oil suspension of S1 nanoparticles under various electric field strengths, *E*, (kV·mm^{-1}): (a) 0, (b) 1.5.

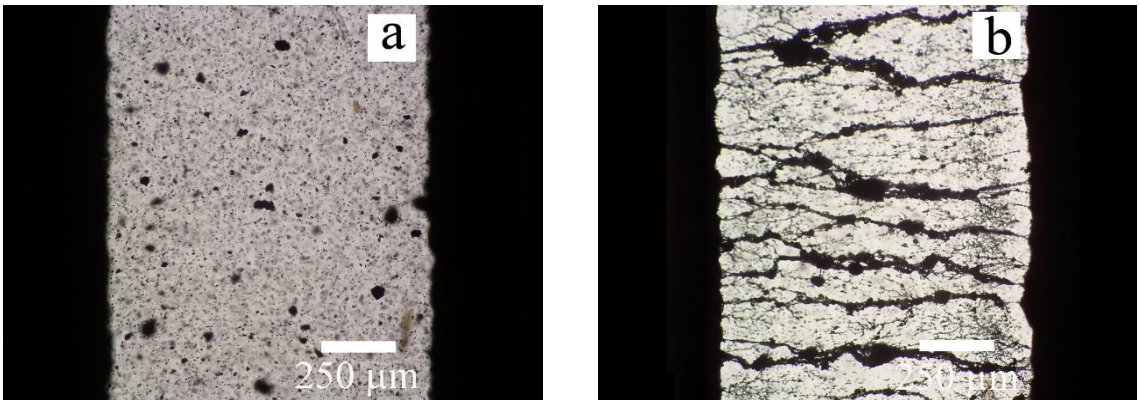

Fig. 12 Optical microscopy of 1 wt% silicone oil suspension of S2 nanoparticles under various electric field strengths, *E*, (kV·mm^{-1}): (a) 0, (b) 1.5.

Conclusions

In this paper the simple and fast preparation of lithium titanate nanoparticles via microwave-assisted molten-salt synthesis was presented. In order to improve the behaviour of the bare lithium titanate nanoparticles under applied external electric field, these particles were coated with urea. It was observed that a suspension based on urea-coated particles exhibits a higher yield stress in two orders of magnitude in comparison to the bare ones. The higher particle concentration in the suspensions, the higher electrorheological effect was exhibited. While the relaxation times of the suspensions were nearly the same for both, the dielectric relaxation strength was two times higher for the suspension based on urea-coated particles than for the suspension based on the bare ones. This explains the increased electrorheological effect of the suspension based on urea-coated particles. Optical microscopy observation provides images well-corresponding with the previous electrorheological findings and consequently shows the suitability of the presented method for the preparation of electrically polarizable particles from TiO_2 anatase nanoparticles for novel ER suspension.

Acknowledgement

This article was written with the support of the Operational Program Research and Development for Innovations co-funded by the European Regional Development Fund (ERDF) and the national budget of the Czech Republic, within the framework of the project of the Centre of Polymer Systems (reg. number: CZ.1.05/2.1.00/03.0111). Author T.P. further thanks an internal grant from TBU in Zlin, No. IGA/FT/2013/014, funded from specific university research resources.

References

(1) Alanis E, Romero G, Martinez C, Alvarez L, Mechetti M. Characteristic times of microsturcture formation in electrorheological fluids, determined by viscosity and speckle activity measurements. *Appl. Rheol.* **2005**, 15(1), 38-45.
(2) Block H, Kelly JP. Electro-Rheology. *J. Phys. D-Appl. Phys.* **1988**, 21(12), 1661-77.
(3) Gast AP, Zukoski CF. Electrorheological Fluids as Colloidal Suspensions. *Adv. Colloid Interface Sci.* **1989**, 30(3-4), 153 -202.
(4) Hao T. Electrorheological fluids. *Adv. Mater.* **2001**, 13(24), 1847-57.
(5) Menna TJ, Filisko FE, Lynch RA. Effect of electric fields on the rheological properties of the isotropic phase of phic/p-xylene solutions. *Appl. Rheol.* **2005**, 15(3), 172-6.

(6) Stenicka M, Pavlinek V, Sahaha P, Blinova NV, Stejskal J, Quadrat O. Electrorheology of suspensions of variously protonated polyaniline particles under steady and oscillatory shear. *Appl. Rheol.* **2010**, 20(5), 1-11.
(7) Schneider S, Eibl S. Review of the electrorheological (ER) effect of polyurethane-based ER fluids. *Appl. Rheol.* **2008**, 18(2), 8.
(8) Plachy T, Sedlacik M, Pavlinek V, Trchová M, Morávková Z, Stejskal J. Carbonization of aniline oligomers to electrically polarizale particles and their use in electrorheology. *Chem. Eng. J.* **2014**, 256, 398-406.
(9) Parthasarathy M, Klingenberg DJ. Electrorheology: Mechanisms and models. *Mater. Sci. Eng. R.* **1996**, 17(2), 57-103.
(10) Tang H, Zhao XP, Wang BX, Zhao Y. Response characteristics of a viscoelastic gel under the co-action of sound waves and an electric field. *Smart Mater. Struct.* **2006**, 15(1), 86-92.
(11) Weiss KD, Carlson JD, Nixon DA. Viscoelastic Properties of Magnetorheological and Electrorheological Fluids. *J. Intell. Mater. Syst. Struct.* **1994**, 5(6), 772-5.
(12) Hong CH, Choi HJ. Shear stress and dielectric analysis of H3PO4 doped polyaniline based electrorheological fluid. *J. Macromol. Sci. Part B-Phys.* **2007**, 46(4), 683-92.
(13) Cheng QL, Pavlinek V, He Y, Yan YF, Li CZ, Saha P. Template-free synthesis of hollow poly(o-anisidine) microspheres and their electrorheological characteristics. *Smart Mater. Struct.* **2011**, 20(6), 6.
(14) Choi SB, Choi HJ, Choi YT, Wereley NM. Preparation and mechanical characteristics of poly(methylaniline) based electrorheological fluid. *J. Appl. Polym. Sci.* **2005**, 96(5), 1924-9.
(15) Lengalova A, Pavlinek V, Cheng QL, Saha P. Increasing electrorheological response of particles: The effect of conductive polymer. *Int. J. Mod. Phys. B.* **2007**, 21(28-29), 4883-9.
(16) Pavlinek V, Saha P, Perez-Gonzalez J, de Vargas L, Stejskal J, Quadrat O. Analysis of the yielding behavior of electrorheological suspensions by controlled shear stress experiments. *Appl. Rheol.* **2006**, 16(1), 14-8.
(17) Stenicka M, Pavlinek V, Saha P, Blinova NV, Stejskal J, Quadrat O. Structure changes of electrorheological fluids based on polyaniline particles with various hydrophilicities and time dependence of shear stress and conductivity during flow. *Colloid Polym. Sci.* **2011**, 289(4), 409-14.
(18) Stenicka M, Pavlinek V, Saha P, Blinova NV, Stejskal J, Quadrat O. The effect of compatibility of suspension particles with the oil medium on electrorheological efficiency. *J. Intell. Mater. Syst. Struct.* **2012**, 23(9), 1055-9.
(19) Cheng QL, Pavlinek V, He Y, Lengalova A, Li CZ, Saha P. Structural and electrorheological properties of mesoporous silica modified with triethanolamine. *Colloids Surf., A.* **2008**, 318(1-3), 169-74.
(20) Cheng QL, Pavlinek V, He Y, Yan YF, Li CZ, Saha P. Synthesis and electrorheological characteristics of sea urchin-like TiO_2 hollow spheres. *Colloid Polym. Sci.* **2011**, 289(7), 799-805.
(21) Liu YD, Choi HJ. Electrorheological fluids: smart soft matter and characteristics. *Soft Matter*. **2012**, 8(48), 11961-78.
(22) Mrlik M, Pavlinek V, Saha P, Quadrat O. Electrorheological Properties of Suspensions of Polypyrrole-Coated Titanate Nanorods. *Appl. Rheol.* **2011**, 21(5), 7.
(23) Zhao XP, Yin JB. Advances in electrorheological fluids based on inorganic dielectric materials. *J. Ind. Eng. Chem.* **2006**, 12(2), 184-98.
(24) He Y, Cheng QL, Pavlinek V, Li CZ, Saha P. Synthesis and electrorheological characteristics of titanate nanotube suspensions under oscillatory shear. *J. Ind. Eng. Chem.* **2009**, 15(4), 550-4.

(25) Cheng QL, Pavlinek V, He Y, Li CZ, Saha P. Electrorheological characteristics of polyaniline/titanate composite nanotube suspensions. *Colloid Polym. Sci.* **2009**, 287(4), 435-41.
(26) Yin JB, Zhao XP. Preparation and electrorheological characteristic of Y-doped BaTiO3 suspension under dc electric field. *J. Solid State Chem.* **2004**, 177(10), 3650-9.
(27) Yin JB, Zhao XP. Titanate nano-whisker electrorheological fluid with high suspended stability and ER activity. *Nanotechnology*. **2006**, 17(1), 192-6.
(28) Lee BM, Kim JE, Fang FF, Choi HJ, Feller JF. Rectangular-Shaped Polyaniline Tubes Covered with Nanorods and their Electrorheology. *Macromol. Chem. Phys.* **2011**, 212(21), 2300-7.
(29) Kozakova Z, Mrlik M, Sedlacik M, Pavlinek V, Kuritka I. Preparation of TiO_2 Powder by Microwave-Assisted Molten-Salt Synthesis. Nanocon 2011. Slezska: Tanger Ltd 2011, p. 345-51.
(30) Sedlacik M, Mrlik M, Kozakova Z, Pavlinek V, Kuřitka I. Synthesis and electrorheology of rod-like titanium oxide particles prepared via microwave-assisted molten-salt method. *Colloid Polym. Sci.* **2012**, 290(2), 1-7.
(31) Lu ZY, Wang YL, Wu WJ, Li YX. Morphology and structure of $LiNb_{0.6}Ti_{0.5}O_3$ particles by molten salt synthesis. *J. Alloy. Compd.* **2011**, 509(40), 9696-701.
(32) Zhang ZQ, Liu ZF, Li YX. Influence of synthesis conditions on the microstructure of Li-Ta-Ti-O microsheets by molten salt method. *Ceram. Int.* **2014**, 40(2), 3747-53.
(33) Cheng QL, He Y, Pavlinek V, Li CZ, Saha P. Surfactant-assisted polypyrrole/titanate composite nanofibers: Morphology, structure and electrical properties. *Synth. Met.* **2008**, 158(21-24), 953-7.
(34) Liu YD, Lee BM, Park TS, Kim JE, Choi HJ, Booh SW. Optically transparent electrorheological fluid with urea-modified silica nanoparticles and its haptic display application. *J. Colloid Interface Sci.* **2013**, 404, 56-61.
(35) Cheng QL, Pavlinek V, He Y, Li CZ, Lengalova A, Saha P. Facile fabrication and characterization of novel polyaniline/titanate composite nanotubes directed by block copolymer. *Eur. Polym. J.* **2007**, 43(9), 3780-6.
(36) Brack W, Heine B, Birkhold F, Kruse M, Schoch G, Tischer S, et al. Kinetic modeling of urea decomposition based on systematic thermogravimetric analyses of urea and its most important by-products. *Chem. Eng. Sci.* **2014**, 106, 1-8.
(37) Havriliak.S, Negami S. A Complex Plane Representation of Dielectric and Mechanical Relaxation Processes in Some Polymers. *Polymer*. **1967**, 8(4), 161-72.
(38) Mrlik M, Sedlacik M, Pavlinek V, Bober P, Trchova M, Stejskal J, et al. Electrorheology of aniline oligomers. *Colloid Polym. Sci.* **2013**, 291(9), 2079-86.
(39) Liu YD, Kim J, Ahn WS, Choi HJ. Novel electrorheological properties of a metal-organic framework Cu-3(BTC)(2). *Chem. Commun.* **2012**, 48(45), 5635-7.
(40) Davis LC. Time-dependent and nonlinear effects in electrorheological fluids. *J. Appl. Phys.* **1997**, 81(4), 1985-91.
(41) Kim SG, Lim JY, Sung JH, Choi HJ, Seo Y. Emulsion polymerized polyaniline synthesized with dodecylbenzenesulfonic acid and its electrorheological characteristics: Temperature effect. *Polymer*. **2007**, 48(22), 6622-31.
(42) Lengalova A, Pavlinek V, Saha P, Quadrat O, Kitano T, Steiskal J. Influence of particle concentration on the electrorheological efficiency of polyaniline suspensions. *Eur. Polym. J.* **2003**, 39(4), 641-5.
(43) Mrlik M, Pavlinek V, Cheng QL, Saha P. Synthesis of Titanate/Polypyrrole Composite Rod-Like Particles and the Role of Conducting Polymer on Electrorheological Efficiency. *Int. J. Mod. Phys. B.* **2012**, 26(2), 8.

(44) Yin JB, Zhao XP. Electrorheological properties of titanate nanotube suspensions. *Colloids Surf., A.* **2008**, 329(3), 153-60.
(45) Zhang WL, Liu YD, Choi HJ, Kim SG. Electrorheology of Graphene Oxide. *ACS Appl. Mater. Interfaces.* **2012**, 4(4), 2267-72.

aTable of Contents Graphic and Synopsis

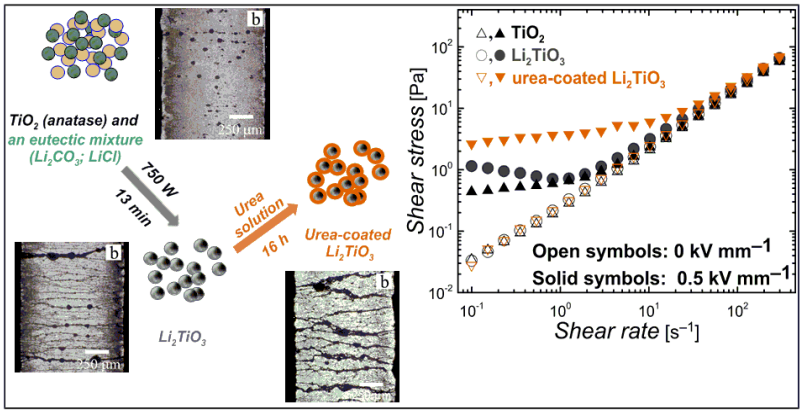

- The lithium titanate nanoparticles were prepared via rapid and environmentally-friendly microwave-assisted molten-salt synthesis
- The lithium titanate nanoparticles were coated with urea
- Urea-coated nanoparticle-based suspension exhibits higher ER performance compare to bare particle-based one